JOURNAL OF MATERIALS SCIENCE 32 (1997) 3283–3291

Formation and undercooling of droplets in the primary phase of Ag–Ge alloys

O. P. PANDEY
School of Basic and Applied Sciences, Thapar Institute of Engineering and Technology, Patiala 147 001, India

S. N. OJHA
Centre of Advance Study, Department of Metallurgical Engineering, Banaras Hindu University, Varanasi 221 005, India

The formation of micro-sized droplets in the matrix of the primary phase of Ag–Ge alloys and their undercooling behaviour were investigated. Thermal cycling consisted in equilibration of hypoeutectic alloys near the eutectic temperature in the two-phase liquid–solid region followed by up-quenching of alloys at 30–50 °C above the eutectic temperature and their subsequent slow cooling. A wide size range of droplets was generated in the matrix of the silver-rich phase by repeated thermal cycling of the alloy. During slow cooling, droplets of silver-rich liquid exhibited a maximum undercooling of 81 °C below the eutectic temperature. Examination of the solidification structure of the undercooled alloys, by X-ray diffraction, polarized light microscopy and electron probe micro analysis techniques, indicated the presence of a metastable phase. The mechanism of formation of droplets and the nature of non-equilibrium solidification of the undercooled melt of silver–germanium alloys, are discussed.

1. Introduction

The role of undercooling in the formation of metastable phases during solidification of metallic melts is well established [1–3]. Currently, there are several techniques available to achieve a large nucleation undercooling of the melt. The principle of undercooling techniques is based on either fluxing the melt in a suitable glass slag [4–6] or subdivision of the melt into small-sized droplets [7–10]. Either way, the heterogeneous nucleants are isolated in a small volume of the melt. One of the variants of the undercooling techniques employing melt subdivision originates from the pioneering work of Wang and Smith [11]. In their work, hypo-eutectic alloys were annealed in the two-phase liquid–solid region. In the process, the liquid film, initially generated along the grain-boundary region, migrated to form isolated droplets in the matrix phase.

It was unambiguously established that isolated liquid droplets, formed within the solid matrix, exhibited larger undercooling compared to the liquid forming a continuous grain-boundary network [12]. Recently, this process has been exploited to study the formation of metastable phases from the undercooled melt of several alloy systems [13–17]. Although the undercooling of the melt depends on the size and size distribution of droplets in the matrix, a systematic study of the formation of isolated droplets in the matrix of its primary phase is still required.

Small-sized droplets in hypo-eutectic alloys can be generated either by slow heating or rapid heating of the alloy and holding them in the two-phase liquid–solid region [12, 18]. During slow heating of the alloys, melting occurs first at grain boundaries and at their triple junctions and the liquid migrates under the influence of temperature and concentration gradients, giving rise to the formation of isolated droplets in the solid phase [14]. In the case of rapid heating, apart from the grain-boundary liquid, homogeneously distributed liquid droplets are also generated within the matrix [20]. The extra solute from the matrix diffuses to these homogeneously distributed droplets and grain-boundary liquid.

The droplets, which are generated by incipient fusion, are found to be very close to each other, thus providing an easy path for solute diffusion [21]. In the case of rapid heating, homogenization has been reported to complete in 1 s in the case of Ag–In alloys [22]. During the course of prolonged holding, these droplets further grow to a large size. Migration of the grain-boundary liquid was reported to be less in the case of rapid heating as compared to that in slow heating for the Al–In system. Young and Clyne [18] also reported the formation of droplets as a result of solute supersaturation in the Al–Mg system annealed and up-quenched in the liquid–solid region. The droplets were observed to be homogeneously distributed in the interior of the grain. These droplets were found to

0022–2461

be less potent for nucleation as compared to the liquid along the grain boundaries.

Keeping these studies of droplet formation in mind, an investigation was planned to study the effect of superheat as well as heating rate on the generation of fine droplets in Ag–Ge alloys. This work also facilitated a study of the undercooling behaviour of liquid entrained in its primary phase, either as continuous film or isolated droplets in this system. The nature of non-equilibrium solidification of undercooled droplets of Ag–Ge alloys is reported.

2. Experimental procedure

2.1. Alloy preparation

The hypo-eutectic silver–germanium alloys containing 10 and 15 at % germanium were made by melting 99.999% purity constituents in a graphite crucible. The melting was carried out in a graphite crucible under the cover of argon gas in an electrical resistance heating furnace. The melt was stirred with a graphite rod and homogenized for some time before pouring in a cylindrical graphite mould of 6.5 mm diameter to achieve effective chilling and thus to avoid segregation. From the as-cast alloys, samples of 8 mm length were cut for thermal cycling and undercooling experiments. Several small-sized samples of 2.5 mm diameter $\times$ 2 mm height were also machined from the as-cast Ag–10 at % Ge alloy to study the formation and undercooling behaviour of droplets in the matrix under controlled thermal cycles in a differential thermal analyser (DTA).

2.2. Thermal cycles and undercooling procedure

The experimental procedure used for generating droplets in the matrix of the primary phase of hypo-eutectic alloy is described elsewhere [17]. In brief, a vertical resistance heating furnace with $\pm$ 2 °C temperature control was used for thermal cycling of the alloys. The heating and cooling rate of the furnace was varied by monitoring the input voltage employing a voltage-controller device. The sample was placed in a silica tube connected to a vacuum pump. A chromel–alumel thermocouple was inserted into a fine hole drilled at the centre of the sample. The other end of the thermocouple was connected to a highly sensitive microvoltmeter. The silica tube was partially evacuated to a vacuum of 10^{-3} torr (1 torr = 133.322 Pa) and back-filled with argon gas. This process was repeated to remove the oxygen gas from the tube. The sample was slowly heated up to a temperature 10 °C above the eutectic temperature of the alloy, and held in the two-phase liquid–solid region for 5–30 min to equilibrate the solid and liquid phases of the alloy. Subsequently, the sample was up-quenched to 30 °C above the eutectic temperature and slowly cooled to a temperature sufficiently below its eutectic temperature. The above thermal cycle was consecutively repeated three times. During the cooling cycle, the time for each 0.1 mV decrease in thermocouple output corresponding to a 2.4 °C drop in temperature, was recorded. The output data with respect to the melting point of the eutectic during the heating cycle were used to calibrate the thermocouple to ensure an accuracy of $\pm$ 1 °C in measurement of temperature. The data generated during the cooling cycle were used to plot the inverse rate cooling curve to identify the thermal peaks corresponding to the nucleation temperature of the melt. In subsequent experiments, the sample was effectively quenched directly from the holding temperature. These samples are referred to as mushy-quenched alloy in further discussions.

The other set of controlled experiments on small-sized samples were performed in a DTA. In this experiment, the sample was heated at a rate of 15 °C min^{-1} up to 655 °C, i.e. 4 °C above the eutectic temperature, held there for 15 min and then up-quenched in the liquid–solid region to 673 °C at a rate of 50 °C min^{-1}. After holding for 2–10 min at the higher temperature, the samples were directly cooled at a rate of 50 °C min^{-1} to a temperature sufficiently below the eutectic temperature. The above thermal cycle was repeated three times for some samples with variation in holding time at the upper temperature, i.e. 673 °C. All thermal cycle data were recorded on an X–Y strip chart recorder.

2.3. Microstructural examination

The samples for the microstructural examination were prepared using standard grinding and polishing techniques. These were etched with an etchant consisting of a saturated solution of potassium dichromate 100 ml, saturated solution of sodium chloride 2 ml, and concentrated sulphuric acid 10 ml. The details of the microstructural features were examined in a Metallux-3 optical microscope. The size and size distribution of droplets in the matrix were determined using a VIDS image analyser. Some of the samples were also examined by polarized light microscopy to study the variation in contrast with a change in polarizing angle. This technique was basically aimed at detecting the metastable phases induced by undercooling of the melt. The constitution of phases and distribution of solute in different regions of the sample were studied in an electron probe microanalyser (EPMA) model JC XA 733 operating at 25 kV. The samples were examined in both the back-scattered as well as secondary electron image mode. The X-ray images of silver and germanium and their line profiles were also recorded. The X-ray diffraction study was performed in a Rigaku X-ray diffractometer using CuK_α radiation. The decomposition behaviour and resultant metastability of phases in heat-treated alloys were also studied.

2.4. Heat treatment

The mushy-quenched alloys were subjected to heat treatment at various temperatures, e.g. 50, 100, 150 and 200 °C, to study the decomposition behaviour of metastable phases. The samples were sealed in an evacuated Pyrex glass tube. The heat treatment was carried out in a resistance heating furnace with $\pm$ 2 °C

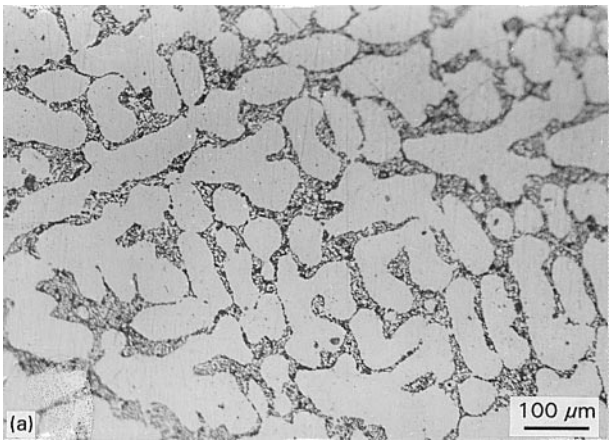

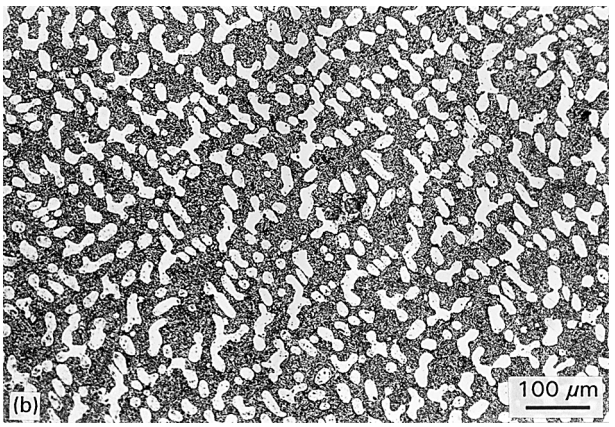

Figure 1 Microstructure of the as-cast alloy showing a continuous network of eutectic in the intergranular region: (a) Ag–10 at % Ge alloy, (b) Ag–15 at % Ge alloy.

temperature control. The isothermal holding time was consistently maintained for 1 h in each experiment. Subsequently the samples were slowly cooled to room temperature. The microhardness measurements of the mushy-quenched and heat-treated samples were carried out using a Tukon microhardness tester employing a load of 50 g.

3. Results and discussion

3.1. Generation of droplets in the matrix

Fig. 1a and b shows the microstructure of the as-cast Ag–10 and 15 at % Ge alloys, respectively. The primary phase has clear granular structure with the intergranular region consisting of the eutectic phases. The eutectic regions also appear to form a continuous network. Annealing of these alloys in the two-phase (liquid + solid) region of the phase diagram of this alloy system gives rise to discontinuity in the distribution of the liquid phase. Samples annealed for a short time exhibited a distinct network of intergranular liquid in the Ag–10 at % Ge alloy. However, in the case of Ag–15 at % Ge alloy, there was a considerable discontinuity in the liquid phase on subsequent annealing. Thus, it appears that the solute concentration of the liquid phase plays a significant role in the migration of the liquid. Repeated melting and freezing cycles of the intergranular phase from the two-phase liquid–solid region to well below the eutectic temperature, leads to the formation of isolated liquid pockets in the primary phase matrix. The thermal cycling experiments on the bulk samples showed many interesting features. The microstructures of the samples which were up-quenched are shown in Fig. 2a–c. Formation of isolated droplets within the grains can be distinctly noticed. However, the size of such droplets appears to depend upon the time of equilibration in the two-phase liquid–solid region and the number of thermal cycles of the specimen. As mentioned earlier, the alloy was initially equilibrated just above the eutectic temperature, whereas the final temperature was 30–50 °C above the eutectic temperature.

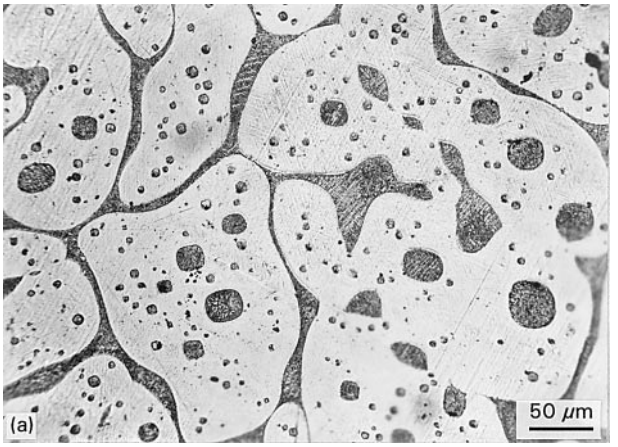

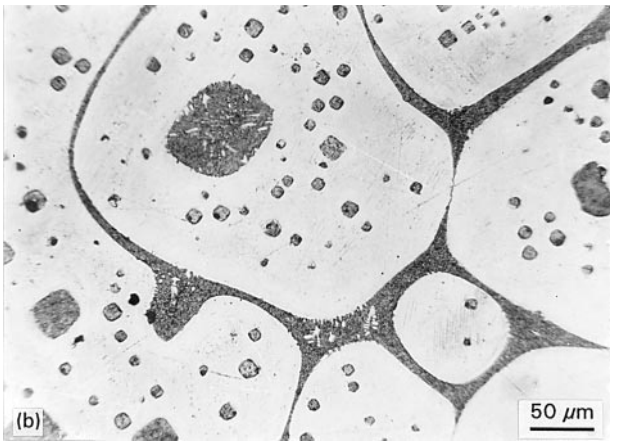

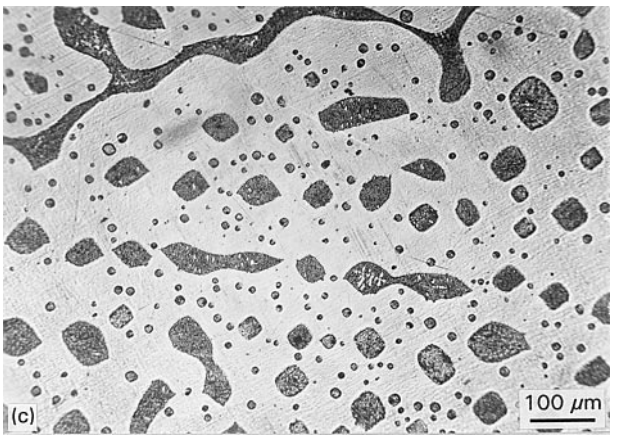

Figure 2 Microstructure of Ag–15 at % Ge alloy after thermal cycling of the bulk sample showing (a) co-existing droplets and grain-boundary phase, (b) a regular geometrical arrangement of fine droplets around larger ones, and (c) the different shape of droplets.

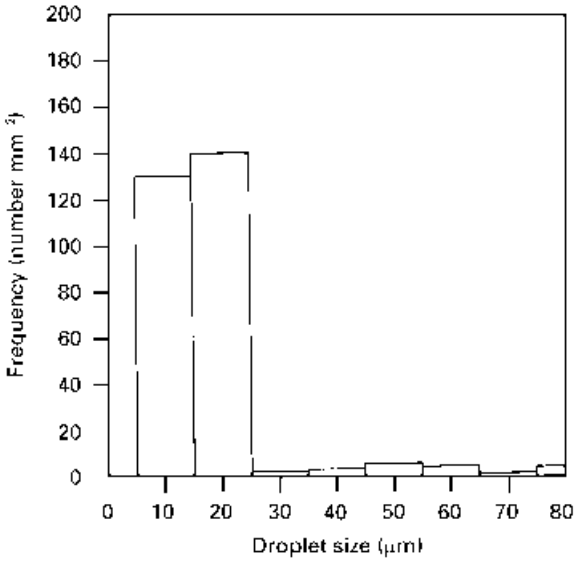

Figure 3 Histogram showing size distribution of droplets in Ag–15 at % Ge alloy.

Interestingly, after the first thermal cycling, according to this schedule, the droplets size is fairly uniform. Nevertheless, after repeated thermal cycling, a wide size range of droplets can be noticed in the micrographs presented in Fig. 2a–c.

It is worthwhile to note that the larger-sized droplets are generally surrounded by finer droplets in a regular pattern. The regions adjacent to the larger droplets are depleted of solute. This observation suggests that the larger droplets act as a source for the formation of finer droplets. The size distribution of droplets determined after three consecutive thermal cycles is shown in Fig. 3. It is difficult to separate at this stage the fraction of droplets formed by migration of liquid or by incipient melting resulting from large supersaturation during the up-quenching process. However, owing to the relatively slow up-quenching rates ($\approx 10\,^{\circ}\mathrm{C\,min^{-1}}$) employed in the thermal cycles of the bulk samples, both mechanisms may operate simultaneously.

In order to understand this effect, subsequent experiments were carried out on small samples (0.17 g) in a differential thermal analyser (DTA). The micrographs taken from these samples are shown in Fig. 4a and b. In these experiments, the holding times at two temperatures, namely, just above the eutectic and the up-quenching temperatures, were less than 10 min. It is worth noting that very fine droplets of uniform size appear in the matrix of the primary phase after the first thermal cycle (Fig. 4a). Increasing the holding time at the up-quenching temperature led to an increase in size of the droplets. In addition, considerable variation in droplet size and size distribution was observed in the samples subjected to a number of thermal cycles. The finer droplets disappear, whereas the larger ones grow further. These effects are shown in the micrograph presented in Fig. 4b. These were taken from the samples subjected to three thermal cycles according to the schedule described earlier. The number frequency curve of the size distribution of droplets is shown in Fig. 5. It is worthwhile to compare the number density of droplets in small and large samples presented in Figs 3 and 5. A large number density of droplets in samples thermally cycled in DTA clearly indicates the mechanism of their formation by incipient melting of the liquid, possibly at defects in the primary phase.

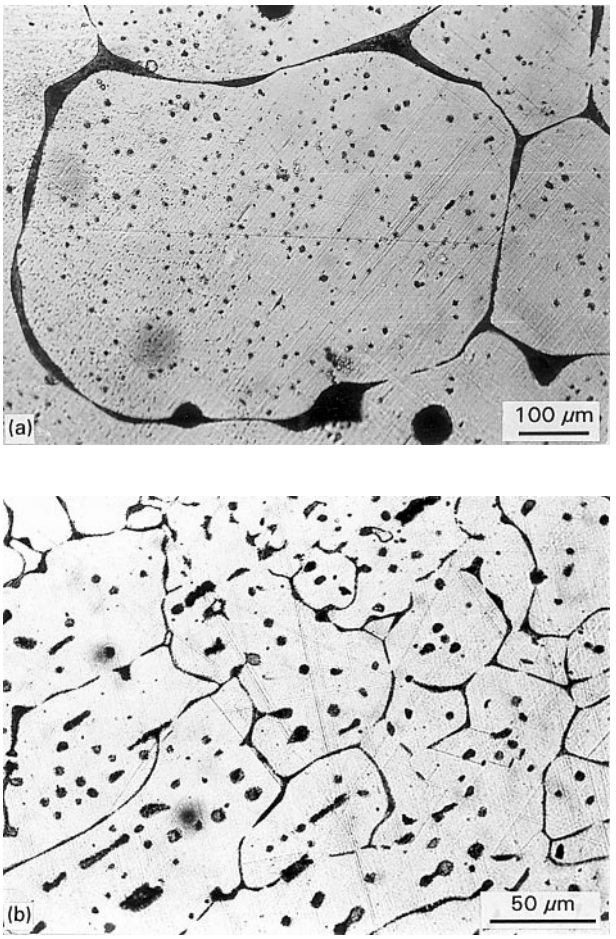

Figure 4 Microstructure of a small sample of Ag–10 at % Ge alloy thermally cycled in a DTA showing (a) fine dispersion of droplets, and (b) coarsening of droplets with increased time of equilibration.

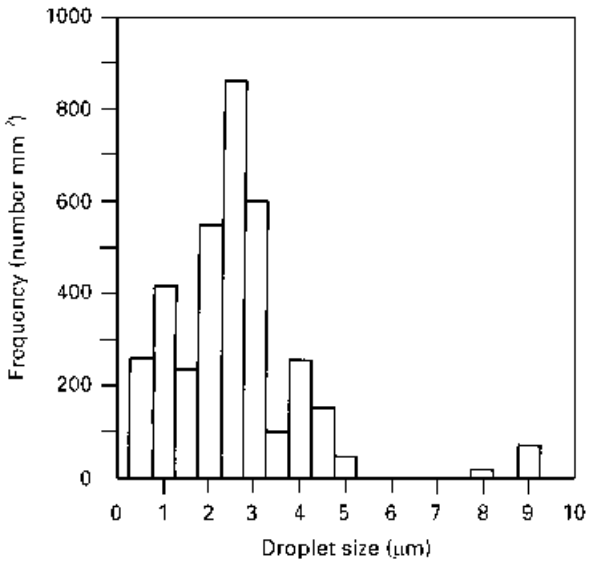

Figure 5 Histogram showing the size distribution of droplets of Ag–10 at % Ge alloy thermally cycled in the DTA.

The nucleation of liquid globules inside the crystals has been attributed either to the presence of micropores in interdendritic sites [20] or to the existence of cyrstalline defects in a constitutionally superheated region near the solid–liquid during melting of a single-phase alloy under high temperature gradients [23]. These investigations also noted that a zone devoid of droplets exists adjacent to most grain boundaries. A common aspect of this study is the population of the existence of a solute-rich domain in the crystal at locations close to the crystal–melt boundary. Recently, Young and Clyne [18] studied the problem of liquation inside grains in slurries prepared for rheocasting. The liquation was attributed to the presence of a supersaturated domain inside the crystal. This model explains simultaneously the role of solid-state supersaturation, the presence of defects and the existence of a droplet-free zone.

The thermal cycle employed in the present work is based on Young and Clyne's model [18]. Accordingly, holding the sample just above the eutectic temperature causes equilibration of the solid and liquid phases. On up-quenching, the system attempts to equilibrate again by partial melting of the solid. This process occurs due to low supersaturation of the solid at the up-quenched temperature. In the absence of back-diffusion in the solid, however, a supersaturated region is created. If the upper temperature is within a range where the driving force due to supersaturation is capable of nucleating liquid on the crystal defects or other inhomogeneities, then nucleation of droplets would occur. Experiments have been designed basically to provide these necessary conditions in both Ag–10 at % Ge and Ag–15 at % Ge alloys. The discontinuity in the histogram (Figs 3 and 5), the periodic peaks and the appearance of peaks of progressively lower size with increasing number of thermal cycles, taken together with the microstructure, indicate that supersaturation around each liquid pocket is responsible for fresh nucleation of entrapped melts. The present study shows that a judicious combination of holding time and up-quenching temperature ensures production of liquid pockets inside the primary phase of this alloy.

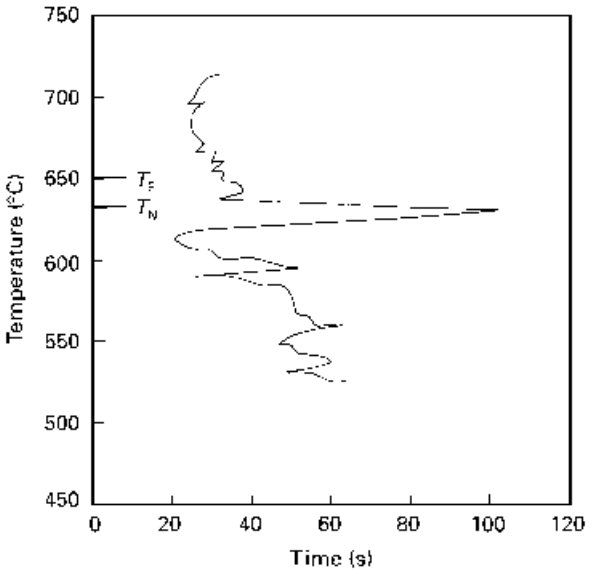

Figure 6 Inverse rate cooling curve of Ag–10 at % Ge alloy.

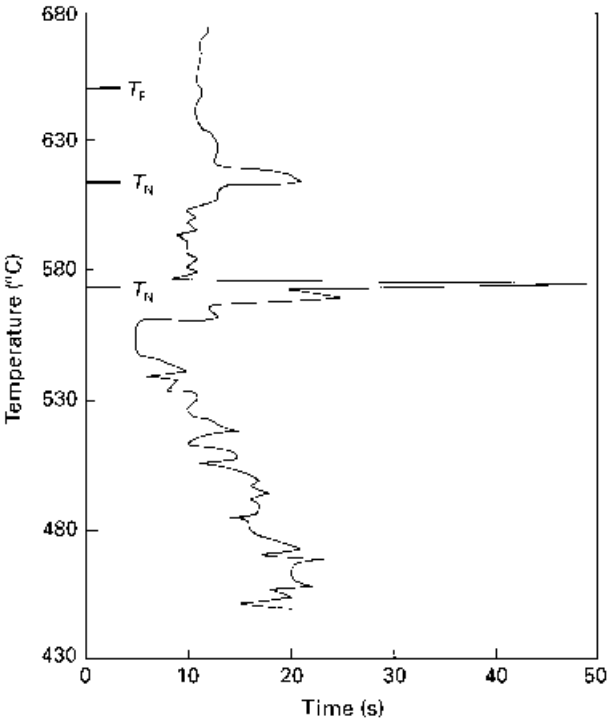

Figure 7 Inverse rate cooling curve of Ag–15 at % Ge alloy.

3.2. Undercooling of droplets

In the present investigation, the samples containing isolated droplets exhibited large undercooling compared to those showing a continuous network of eutectic. This effect was invariably observed in both the small and bulk samples. A typical inverse rate cooling curve obtained from bulk samples of Ag–14 at % Ge alloy is shown in Fig. 6. This was obtained after repeated thermal cycling of the alloy. A large nucleation peak around 630 °C can be noticed, besides several small peaks at lower temperatures. The large peak may be considered to arise due to freezing of large-sized droplets, whereas smaller peaks correspond to nucleation of smaller-sized droplets. During slow cooling of the sample, the composition of the liquid changes along the liquidus line. Thus, if the thermal peaks are considered as nucleation temperatures of droplets of different size, it amounts to an undercooling of 20 °C below the eutectic temperature which is equivalent to an undercooling of 42 °C below the liquidus temperature of this alloy.

A similar behaviour has also been observed in the bulk samples of Ag–15 at % Ge alloy. However, in this case, the large peak appears around 570 °C with additional small peaks in the temperature range 532–450 °C as shown in Fig. 7. Even nucleation at 570 °C amounts to an undercooling of around 81 °C below the eutectic temperature. Thus droplets containing a higher percentage of germanium appear to undergo larger undercooling in this system. Similar undercooling behaviour of droplets generated in small samples in the DTA study was also observed. After the

first thermal cycle, a broad solidification peak appeared at around 611 °C having a spread of 5 °C. In subsequent thermal cycles, the prominent peak occurred around 600 °C. The nucleation temperature did not change further on subsequent thermal cycling of the sample.

The present investigation demonstrates that large undercooling is possible only in liquid-forming isolated droplets. This observation is consistent with the work of Southin and Chadwick [12]. However, a notable feature of the present study is related to an increase in the undercooling of the melt with increasing thermal cycling of the sample. In addition, the effect of spatial distribution of the liquid in the matrix phase on undercooling of the melt is clearly seen. When the liquid phase forms a continuous network along grain boundaries, even one nucleation event is sufficient to freeze the whole liquid at one time. In contrast, nucleation events are independent in isolated droplets. This behaviour of melt undercooling indicates the importance of controlling the size and size distribution of droplets in the matrix phase. The repeated thermal cycling of the melt is attributed to change in the potency of a nucleant, so that large undercooling is induced in the melt. Although this effect is difficult to characterize in the present study, the earlier investigations on undercooling of a liquid contained in a glass slag have clearly established this behaviour of the melt undercooling [24, 25].

The shape of the droplet and the nature of liquid–solid interface is also likely to control the undercooling behaviour of the melt. It has been earlier shown that any asperities present in the solid–liquid interface induce nucleation in the liquid even at a relatively low undercooling [26]. In the present investigation, the solid–liquid interface had a smooth curvature in the case of droplets whereas the interface was irregular in the case where the liquid formed a continuous network. The nature of the interface depended on the thermal cycling of the alloy from a two-phase liquid–solid region. Thus, thermal cycling of the alloy favours undercooling of the melt in two ways. Firstly it leads to a decrease in size of the droplets, and secondly it generates a smooth curvature of the solid–liquid interface. Consequently, the undercooling of the melt increases in this process.

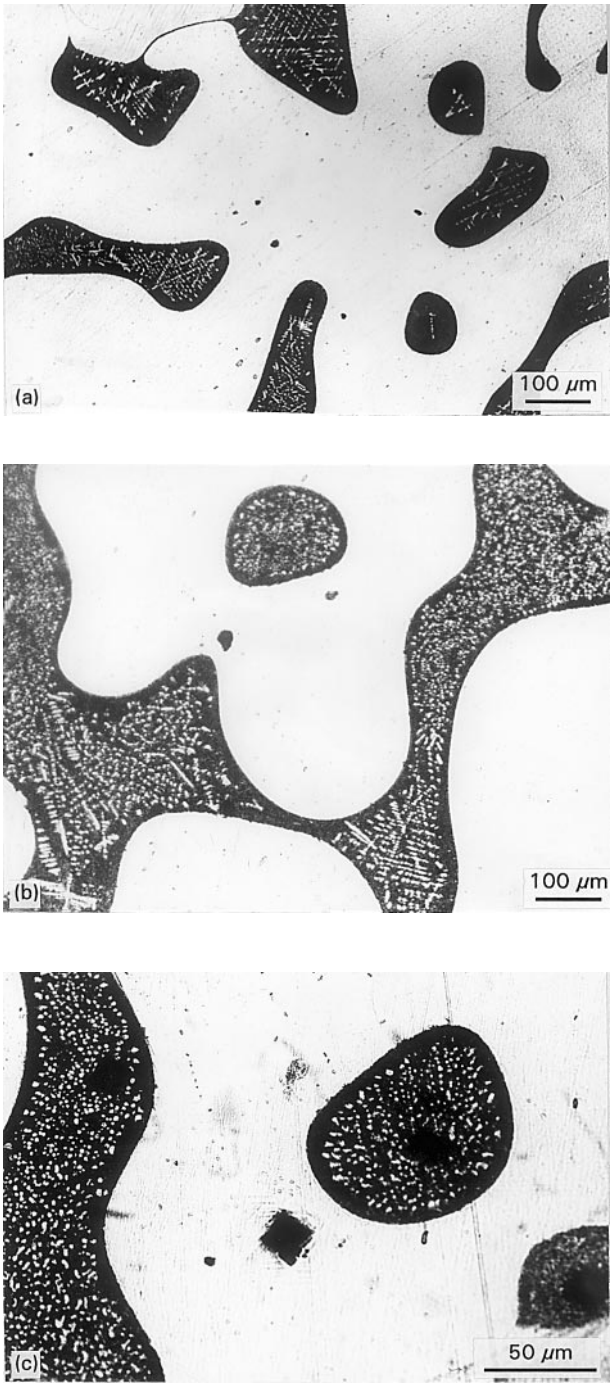

Figure 8 Microstructure of a mushy-quenched Ag–15 at % Ge alloy showing (a) regular arrangement of dendrites of primary phase, (b) co-existing dendritic and spherical morphology, and (c) fully spherical morphology of primary phase in the solidification structure.

3.3. Microstructural features induced by undercooling

The undercooled and mushy-quenched alloy showed several metastable effects. Consequently, these were characterized employing X-ray diffraction, EPMA and hardness measurement techniques. Fig. 8a shows the microstructure of mushy-quenched Ag–15 at % Ge alloy. The prior liquid-phase region in this sample is mostly observed as a continuous network in the inter-granular spaces of the primary phase. It is interesting to observe a large number of small-sized dendrites of the primary phase with a featureless interdendritic region in the solidification structure. The volume fraction of dendrites is noticed to decrease in small-sized droplets, as shown in Fig. 8b. The hardness measurements on the primary phase and the featureless region, exhibited a considerable difference in their hardness values. It is also interesting to observe considerable variation in the morphology of the primary phase formed in the solidification structure of droplets. For example, the morphology of the primary phase changes from a typical dendritic to a spherical shape as shown in Fig. 8c. Such a transition has earlier been observed by several investigators [27, 28]. It was quantitatively shown that the primary phase of Ag–Ge alloy undergoes a typical dendritic to cylindrical to spherical transition as a function of undercooling of the melt. Thus the droplets exhibiting

TABLE I Hardness variation in Ag–14 at % Ge alloy

Sample condition	Hardness (VHN)	
	Matrix	Transformed region
As cast	72	106
Mushy quenched (MQ)	65	167
MQ + HT at 50 °C for 1 hr	45	86
MQ + HT at 150 °C for 1 hr	49	75

MQ: Mushy Quenched; HT: Heat Treated.

spherical morphology in the present work are considered to solidify from a highly undercooled melt in the mushy-quenched alloy. Yet another noteworthy observation is the formation of a featureless region near the droplet–matrix interface. This feature is attributed to a large heat sink provided by the surrounding solid phase to absorb the heat of fusion evolved during solidification of droplets. Consequently, the effect of recalescence is minimized during this stage of solidification and the melt undergoes a diffusionless transformation.

X-ray diffraction of the samples showed reflection only due to the silver-rich phase and germanium. The silver-rich solid-solution phase revealed a lattice parameter of 0.4108 nm. This corresponds to an increase in solubility of nearly 2% of germanium over the equilibrium limit of this alloy. The decomposition of this phase was followed by hardness measurements. A typical variation in hardness values is shown in Table I. The hardness of the matrix phase is 72 VHN compared to 106 VHN for the eutectic region in the as-cast alloy. However, the mushy quenched alloy exhibits a hardness of 65 VHN for the matrix phase in contrast to 167 VHN for the solidification structure of the transformed phase. Samples heat treated from 50–150 °C showed considerable drop in hardness values for both the matrix as well as the transformed region of the mushy-quenched alloy. This hardness variation reflects the decomposition of metastable phases to the equilibrium ones.

The mushy-quenched Ag–10 at % alloy also showed a phase with fine acicular morphology within transformed regions as shown in Fig. 9a–c. The acicular phase was found to be sensitive to the polarized light, as is evident from the above micrographs. This observation clearly indicates the presence of a non-cubic metastable phase in the solidification structure of this alloy. However, identification of this phase is difficult at this stage, because its low volume fraction (in relation to the whole sample) limits its detection by X-ray diffraction. However, a considerable variation in the composition of the acicular phase was observed in the EPMA studies. Fig. 10a–c shows the compositional contrast in the back-scattered mode, corresponding X-ray images of AgK_α radiations and composition profiles of silver- and germanium-rich phases. It is apparent that the acicular phase is silver-rich while the surrounding phase is silver-deficient. Thus the EPMA studies also indicate an altogether different constitution of the acicular phase, although a quantitative analysis of this phase could not be performed due to the small width of the needles and interference of signals of the electron probe from the surrounding phases.

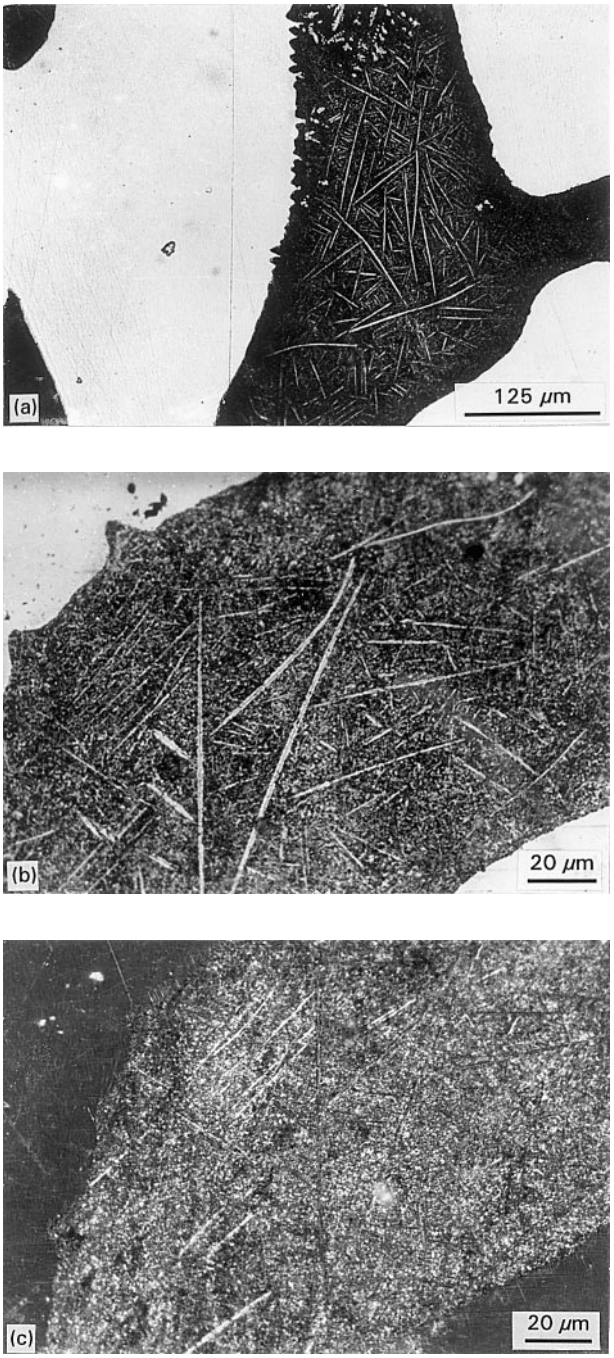

Figure 9 Microstructure of a mushy-quenched Ag–10 at % Ge alloy showing (a) acicular morphology, and (b, c) the effect of polarized light in the contrast of the acicular phase.

Ag–Ge alloys under rapid solidification conditions have reflected the formation of metastable phase with HCP crystal structure [29]. Recently, Pandey [30] presented a thermodynamic justification for the occurrence of a metastable phase in this system. This is based on investigating the stability of the liquid as a function of composition. It was shown that under kinetically induced favourable conditions, nucleation of a single-phase solid with an approximate stoichiometric Ag_3Ge would be easier than the nucleation of independent silver- and germanium-based phases requiring diffusion in the liquid.

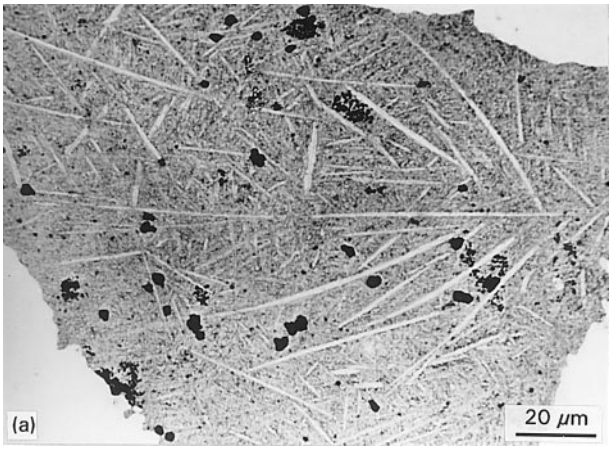

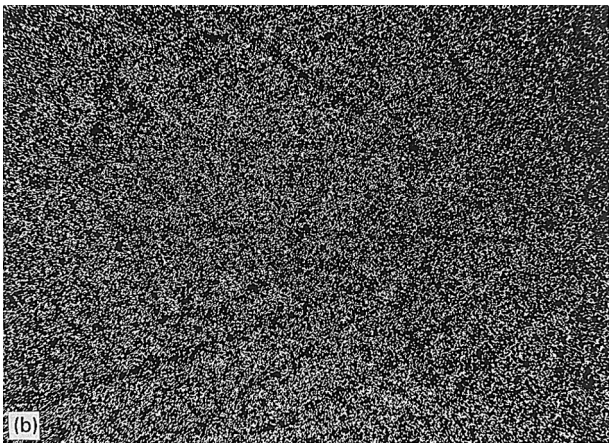

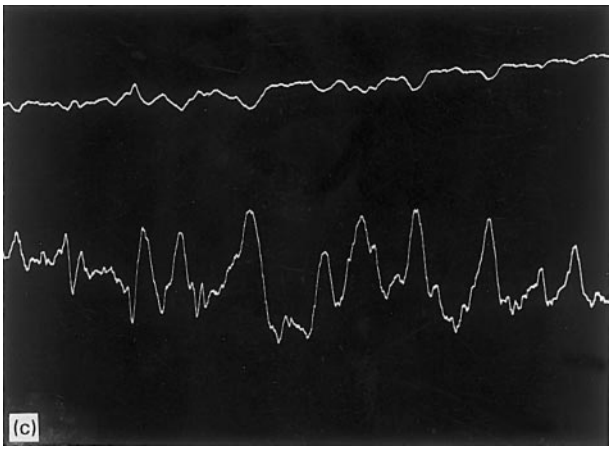

Figure 10 Microstructure of Ag–10 at % Ge alloy: (a) the back-scattered image, (b) the X-ray image of AgK_{α} radiation, and (c) variation in the composition of the matrix and acicular phase.

Although a metastable phase with acicular morphology is indicated in the present work by polarized light microscopy and EPMA study, the volume fraction of the phase is significantly small to confirm whether this is identical to the HCP phase mentioned above.

In summary, the results of the present investigation demonstrate the role of size and size distribution of droplets, generated in the matrix of the primary phase, on the undercooling behaviour of the melt and its subsequent ability to form a metastable phase during solidification.

4. Conclusions

1. Equilibration of hypo-eutectic Ag–Ge alloys in a two-phase liquid–solid region followed by their up-quenching at 40–50 °C above the eutectic temperature, leads to the formation of droplets in the matrix of the primary phase. Thermal cycling of the alloy between the up-quenching temperature to well below the eutectic temperature provides an increase in the size range of droplets. The rate of up-quenching is observed to have a significant effect on the formation of small-sized droplets in this alloy system. The result indicates that the solute-rich liquid acts as a source for further nucleation of droplets around them in the subsequent thermal cycling.

2. Isolated droplets of silver-rich liquid exhibit large undercooling compared to the liquid forming a network in the intergranular region of the primary phase. The maximum undercooling achieved in droplets of Ag–15 Ge alloy is observed to be 81 °C below the eutectic temperature of the alloy. The spatial distribution of droplets in the matrix and change in potency of nucleants during repeated thermal cycling are considered to generate large undercooling of droplets.

3. Microstructural examination of undercooled alloys by X-ray diffraction, polarized light microscopy and EPMA technique indicates the formation of a metastable phase in the solidification structure of undercooled alloys.

Acknowledgements

The authors thank Professor S. Lele, Department of Metallurgical Engineering, Banaras Hindu University, for valuable discussions, and Dr N. S. Mishra, R. and D. Centre, SAIL, Ranchi, for carrying out the electron probe microanalysis of undercooled alloys.

References

1. S. N. OJHA, P. RAMACHANDRARAO and T. R. ANANTHARAMAN, *J. Mater. Sci.* **18** (1983) 1174.
2. J. H. PEREPEZKO, *Mat. Sci. Eng.* **65** (1984) 125.
3. S. N. OJHA, K. CHATTOPADHYAY and P. RAMACHANDRARAO, *ibid.* **73** (1985) 177.
4. G. L F. POWELL, *J. Aust. Inst. Metals* **10** (1965) 223.
5. T. Z. KATTAMIS and M. C. FLEMINGS, *Trans. AIME* **233** (1965) 1662.
6. S. N. OJHA, P. RAMACHANDRARAO and T. R. ANANTHARAMAN, *Trans. Ind. Inst. Metals* **36** (1983) 51.
7. D. TURNBULL, *J. Chem. Phys.* **18** (1950) 198.
8. J. H. PEREPEZKO and D. H. RASMUSSEN, *Metall. Trans.* **9A** (1978) 1490.
9. C. C. LEVI and R. MEHRABIAN, *ibid.* **13A** (1982) 221.
10. O. P. PANDEY and S. N. OJHA, *Powder Met. Int.* **23** (1991) 291.
11. C. C. WANG and C. S. SMITH, *Trans. AIME* **188** (1950) 136.
12. R. T. SOUTHIN and G. A. CHADWICK, *Acta Metall.* **26** (1978) 223.
13. P. RAMACHANDRARAO, K. LAL, A. SINGHDEO and K. CHATTOPADHYAY, *Mater. Sci. Eng.* **41** (1979) 259.
14. Y. V. S. S. PRASAD, P. RAMACHANDRARAO and K. CHATTOPADHYAY, *Acta Metall.* **32** (1984) 1825.
15. K. CHATTOPADHYAY, V. T. SWAMY and S. L. AGARWALA, *Acta Metall. Mater.* **38** (1990) 521.

16. O. P. PANDEY, N. S. MISHRA, C. RAMACHANDRARAO, S. LELE and S. N. OJHA, *Metall. Mater. Trans.* **25A** (1994) 2517.
17. O. P. PANDEY, S. LELE, N. S. MISHRA and S. N. OJHA, *J. Mater. Sci.* **30** (1995) 538.
18. R. M. K. YOUNG and T. W. CLYNE, *Acta Metall.* **37** (1989) 663.
19. W. A. MILLER and G. A. CHADWICK, *Proc. Roy. Soc.* **A312** (1969) 257.
20. S. A. BALA and J. A. LUND, *Z. Metallkde* **70** (1979) 185.
21. Y. E. S. KUCHARENKO, *Fiz. Metall. Metalloved* **39** (1975) 815.
22. T. MUSCHIK, W. A. KAYSSER and T. NEHENKAMP, *Acta Metall.* **37** (1989) 603.
23. J. D. VERNHOVEN and E. D. GIBSON, *J. Cryst. Growth* **11** (1971) 29.
24. G. L. F. POWELL and L. M. HOGAN, *Trans. AIME* **242** (1968) 2133.
25. S. N. OJHA and P. RAMACHANDRARAO, *J. Mater. Sci. Lett.* in press.
26. S. N. OJHA, *Z. Metallkde* **82** (1991) 41.
27. T. Z. KATTAMIS and M. C. FLEMINGS, *Mod. Casting* **52** (1967) 97.
28. S. WALDER and P. L. RYDER, *J. Apply. Phys.* **73** (1993).
29. P. RAMACHANDRARAO and T. R. ANANTHARAMAN, *Philos. Mag.* **20** (1969) 201.
30. O. P. PANDEY, PhD thesis, Banaras Hindu University (1992).

Received 15 September 1995
and accepted 15 January 1996